CHEMICAL ENGINEERING TRANSACTIONS
VOL. 96, 2022
A publication of AIDIC
The Italian Association of Chemical Engineering
Online at www.cetjournal.it
Guest Editors: David Bogle, Flavio Manenti, Piero Salatino

ISBN 978-88-95608-95-2; **ISSN** 2283-9216
DOI: 10.3303/CET2296071

Analysing the Performance of MCECs over a Wide Range of Operating Temperatures

Maria Anna Murmura [a,*], Massimiliano Della Pietra [b], Stefano Frangini [b], Claudia Paoletti [b], Francesca Santoni [b], Maria Cristina Annesini [a]

[a]Department of Chemical Engineering Materials and Environment, University of Rome "La Sapienza", Via Eudossiana 18, 00184, Rome, Italy
[b]ENEA CRE Casaccia, TERIN-PSU-ABI, Via Anguillarese 301, 00123, Rome, Italy
mariaanna.murmura@uniroma1.it

Hydrogen production through water electrolysis has gained significant attention in the past years as a means of tackling the problem of the imbalance between the intermittent rate of electricity production from renewable sources and the continuous electricity demand from end users. Recently, much of the effort has been shifted toward the electrolysis of steam rather than water, for example in solid oxide cells, which operate at temperatures around 800°C. In this manner, part of the energy required for the conversion to hydrogen is provided as heat rather than electricity. At the same time, the high temperature levels require the use of highly resistant materials, which increase the overall cost of the process. An interesting alternative is represented by molten carbonate electrolysis cells (MCECs), operating at temperatures well below 700°C. In the present work, a molten carbonate cell was operated in a lower temperature range (490-550°C) by changing the composition of the electrolyte mixture. The data obtained, along with experimental results at higher temperature (570-650°C) available in the literature, was analyzed using a 0D model accounting for Ohmic and activation overpotentials to determine the correlation between current and potential. It was found that, while the dependence of Ohmic losses on temperatures is discontinuous when cell operation is switched from the lower to the higher temperature range, activation losses vary with continuity. This result provides important insight on the performance of MCECs that can serve as a basis for future studies.

1. Introduction

The electrolysis of water is a well-known process for the conversion of electrical energy into chemical energy and can contribute to reducing the problem of the imbalance between the intermittent rate of electricity production from renewable source and the continuous demand from the grid. In low-temperature electrolysis, the energy required for the conversion of water into hydrogen is exclusively high-value electrical energy. Electrolysis of steam, on the other hand, reduces the demand of electrical energy as some of the power input is in the form of heat. Solid oxide electrolysis cells (SOECs), which operate at temperatures of approximately 800°C, are close to commercialisation; however, the high temperatures require the use of resistant, and therefore expensive, materials. The cathodic and anodic semi-reactions taking place in a SOEC are, respectively,

$$H_2O + 2e^- \rightarrow O^{2-} + H_2 \quad (1)$$

$$O^{2-} \rightarrow \frac{1}{2}O_2 + +2e^- \quad (2)$$

The lower limit on operating temperature is linked to the conductivity of O^{2-} ions in the solid electrolyte (Hauch, 2020).

Paper Received: 22 November 2021; Revised: 19 June 2022; Accepted: 30 September 2022
Please cite this article as: Murmura M.A., Della Pietra M., Frangini S., Paoletti C., Santoni F., Annesini M.C., 2022, Analysing the Performance of Mcecs over a Wide Range of Operating Temperatures, Chemical Engineering Transactions, 96, 421-426 DOI:10.3303/CET2296071

An alternative is represented by molten carbonate electrolysis cells (MCECs), which operate at temperatures around 650°C, thereby reducing the requirements of the materials used for the realization of the cell and other equipment. While molten carbonate cells operating in fuel cell mode are close to commercialization (Audasso, 2022), their operation in electrolysis mode is still at the lab-scale level (Monforti Ferrario, 2021). The cathodic and anodic reactions are

$$H_2O + CO_2 + 2e^- \rightarrow CO_3^{2-} + H_2 \quad (3)$$

$$CO_3^{2-} \rightarrow CO_2 + \frac{1}{2}O_2 + 2e^- \quad (4)$$

In this case, the lower limit on operating temperature depends on both electrolyte mixture melting point and on the conductivity of CO_3^{2-} ions in the liquid electrolyte. More specifically, the melting point of the electrolyte mixture should be at least 100°C lower than the maximum envisaged operating temperatures, to ensure that solidification does not occur, even locally. The most widely studied MCECs employ an electrolyte mixture of Li_2CO_3/K_2CO_3, having an ionic conductivity of 0.8-2 S/cm for temperatures between 500 and 900°C and a melting point of approximately 500°C (Hu, 2016). Recently, the possibility of operating MCECs at temperatures in the range 500-550°C has been proposed (Frangini, 2013); this represents an advantage not only in terms of material requirements, but also because of the potential of coupling the process with medium-scale solar concentrating systems. Working at lower temperatures has been made possible by changing the composition of the electrolyte mixture to a ternary eutectic mixture of $Li_2CO_3/Na_2CO_3/K_2CO_3$, which was found to have a melting point of 397°C while maintaining a high ionic conductivity (0.3-2.5 S/cm between 500 and 900°C (Kojima, 2008)); however, information is still missing regarding the effect of electrolyte composition on the rate of the redox reactions.

In the present work, a lab-scale electrolysis cell was tested with the eutectic mixture of Li/Na/K carbonates at temperatures ranging between 490 and 550°C. The results were analyzed with a so-called 0D model, relating the applied potential to the current density, which takes into account Ohmic and activation losses. The model was also applied to data relative to a high-temperature MCEC available in the literature (Perez-Trujillo, 2018).

2. Experimental

The electrolysis experiments in the low-temperature range of 490-550°C were conducted with the eutectic ternary salt Li_2CO_3-Na_2CO_3-K_2CO_3 (43.5-31.5-25.0 mol%). For the preparation of the mixture, reagent-grade Li_2CO_3, Na_2CO_3 and K_2CO_3 powders were dried overnight at 300°C before being mixed in a roller jar mill at the optimized roller speed of 60 RPM for 24h.

Since our MCFC single cells are assembled with porous electrodes that, according to the supplier information, could operate stably only with the standard Li_2CO_3-K_2CO_3 electrolyte, a different cell arrangement was put up for the electrolysis experiments with the ternary eutectic salt. Thus, the low-temperature electrolysis experiments were conducted in a classical tank cell comprising two electrodes fully immersed in the melt, a micro gas diffuser, a stainless steel top cover and an alumina crucible filled with about 400 g of electrolyte. The cell was heated in a pit-type furnace, to keep the temperature constant during cell operation. Face-to-face planar gold foils each with a surface area of 15 cm^2 were used as electrodes. The distance between the electrodes was 2 cm. A CO_2+H_2O gas mixture (vol ratio 1:1, total gas flow rate=60 ml/min) was bubbled in the electrolyte through a ceramic micro bubble gas diffuser placed near the cathode electrode. A DC power (Manson, Model HCS-3402) and a high-precision digital multimeter (Fluke, Model 77 III) were used for voltage and current measurements, respectively. E-i curves were obtained under voltage control by slowly stepping the voltage between 0.8 and 1.7 Volt. At each step, the reading was taken until the current reached a stable value (usually, after 30 seconds).

Figure 1 reports the E-i curves obtained in the low-temperature range. It can be observed that, in general, both temperature and voltage have a strong effect on the electrolysis current. More in detail, current is seen to sharply increase above 1.2 V with a tendency to further accelerate beyond 1.4 V. Current acceleration is more evident from 520°C upward. The theoretical hydrogen production, evaluated by assuming 100% Faradaic efficiency, varied between 1.9 and 3.5x10^{-3} mmol/(min·cm^2).

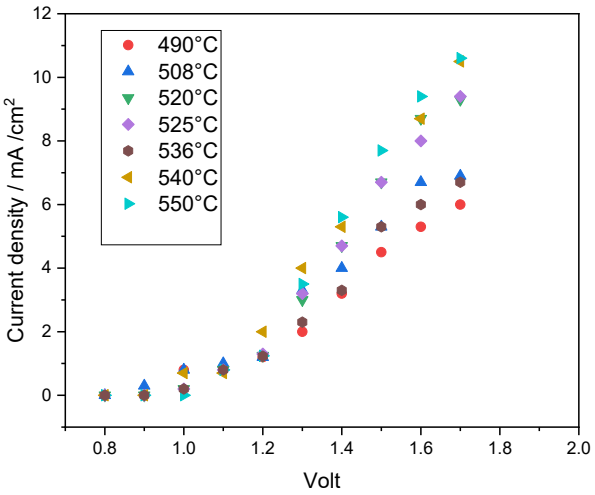

Figure 1 – E-I curves obtained during molten carbonate electrolysis experiments in the low-temperature range.

3. Model development and results

The 0D model was developed by accounting for Ohmic, $\eta_{ohm}(T,i)$, and activation, $\eta_{att}(T,i)$, overpotentials. The total overpotential, $\eta(T,i)$, is therefore given by

$$\eta(T,i) = E_{app} - E_{Nernst}(T,i) = \eta_{ohm}(T,i) + \eta_{att}(T,i) \tag{5}$$

where E_{app} is the applied potential and $E_{Nernst}(T,i)$ is the Nernst potential, which depends on temperature and gas composition according to Eq. (6)

$$E_{Nernst}(T,i) = E_0(T) - \frac{RT}{2F} ln \left(\frac{p_{H_2,cat} \cdot p_{O_2,an}^{1/2} \cdot p_{CO_2,an}}{p_{H_2O,cat} \cdot p_{CO_2,cat}} \right) \tag{6}$$

$E_0(T)$ was evaluated as

$$E_0(T) = -\frac{\Delta G_r^0(T)}{2F} \tag{7}$$

where the expression of $\Delta G_r^0(T)$ was taken from (Reyes Belmonte, 2017), with *T* in *K*

$$\Delta G_r^0(T) = 244800 - 49.18 \cdot T - 2.72 \cdot 10^{-3} \cdot T^2 \text{ J/mol} \tag{8}$$

The gas composition was evaluated by accounting for the composition of the gas fed to the cell; the effect of the electrochemical reaction, related to the current density; and the effect of chemical reactions. For the latter, the reverse-water-gas shift (rWGS) and methanation reactions were considered to take place at high temperatures, whereas only the rWGS reaction was accounted for at lower temperatures. The chemical reactions were considered to be always at equilibrium. More specifically, the effect of the electrochemical reaction was initially accounted for by determining, for each value of the current density, the rate of production/consumption of each component making use of Faraday's law. The rate of hydrogen production was given by

$$F_{H_2,pr}^{cat} = \frac{i \cdot S}{2 \cdot F} \tag{9}$$

where *S* is the geometric surface of the electrode and *F* is Faraday's constant. The corresponding rates of water and carbon dioxide consumed by the cathodic reaction are

$$F_{H_2,pr}^{cat} = F_{H_2O,cons}^{cat} = F_{CO_2,cons}^{cat} \tag{10}$$

Similarly, the rates of carbon dioxide and oxygen produced by the anodic reaction is related to the rate of hydrogen production according to

$$F_{CO_2,pr}^{an} = F_{H_2,pr}^{cat} \tag{11}$$

$$F_{O_2,pr}^{an} = \frac{1}{2} \cdot F_{H_2,pr}^{cat} \tag{12}$$

The resulting compositions were considered as feed to the rWGS/methanation reactions in order to determine the Nernst potential.
Ohmic overpotentials are related to the current density through Ohm's law

$$\eta_{ohm}(T,i) = r(T) \cdot i \tag{13}$$

where $r(T)$ is the Ohmic resistance, which was considered to depend on temperature as the inverse of the ionic conductivity of the electrolyte

$$r(T) = \frac{l}{\sigma(T)} \tag{14}$$

where *l* is a fitting parameter and $\sigma(T)$ is the electrolyte conductivity, whose temperature dependence was provided in (Hu, 2016) for high temperatures (Eq.(15)) and (Kojima, 2008) for low temperatures (Eq.(16))

$$\sigma(T) = -3.2403 + 5.2415 \times 10^{-3}T - 0.2289 \times 10^{-6}T^2 \tag{15}$$

$$\sigma(T) = -2.797 + 4.6115 \times 10^{-3}T - 0.0291 \times 10^{-6}T^2 \tag{16}$$

with *T* in *K* and σ in S/cm.
The activation overpotential was determined from the Butler-Volmer equation

$$i = i_0 \left(exp\left(\alpha_a \frac{nF\eta}{RT}\right) - exp\left(-\alpha_c \frac{nF\eta}{RT}\right)\right) \tag{17}$$

in which the transfer coefficient, α, was considered to be equal to 0.5, from which the following dependence between measured current density, exchange current density (i_0), and temperature, was derived

$$i = 2i_0 sinh\left(\frac{F\eta_{att}}{RT}\right) \tag{18}$$

and therefore

$$\eta_{att} = \frac{RT}{F} arcsinh\left(\frac{i}{2i_0(T)}\right) \tag{19}$$

The values of the exchange current densities, i_0, at each temperature were obtained by fitting the experimental data.
The total overpotential is therefore given by

$$\eta = r(T) \cdot i + \frac{RT}{F} arcsinh\left(\frac{i}{2i_0(T)}\right) \tag{20}$$

Figures 2 and 3 show a comparison between the E-I curves obtained experimentally and from the 0D model in the high and low temperature range, respectively. It should be noted that the data in the high temperature range was obtained by working with a planar cell in which the distance from the electrodes was about 1 mm. The agreement between modelled and experimental results is very good.

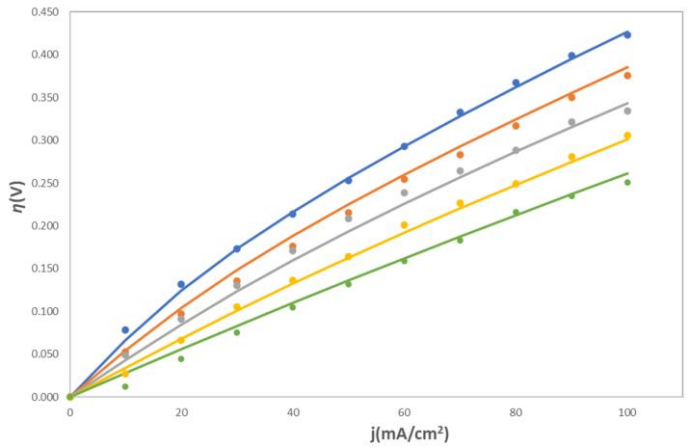

Figure 2: Comparison between experimental (points) and calculated (continuous lines) η-i curves in the high-temperature range. Data was analyzed at temperatures of 570 (blue), 590 (orange), 610 (grey), 630 (yellow), and 650°C (green).

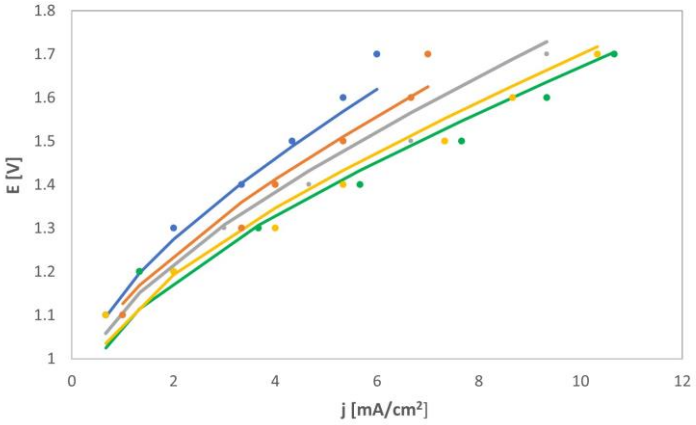

Figure 3: Comparison between experimental (points) and calculated (continuous lines) E-i curves in the low-temperature range. . Data was analyzed at temperatures of 490 (blue), 508 (orange), 520 (grey), 540 (yellow), and 550°C (green).

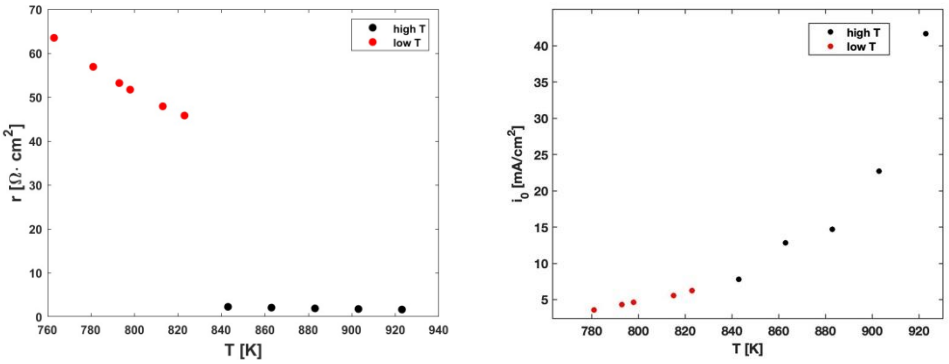

Figure 4. (a) Ohmic resistance and (b) exchange current density obtained by fitting the experimental data at high (black points) and low (red points) temperature.

Figures 4a and b show the Ohmic resistance and exchange current density, respectively, as a function of temperature. It is interesting to note that while there is a discontinuity in the dependence of Ohmic resistance on temperature, the exchange current density shows the same behavior in the high- and low-temperature range. Regarding the discontinuity in the Ohmic resistance, the inverse of the ionic conductivity at 560°C, i.e. the temperature at which the electrolyte composition needs to be modified, is 1 cm/S for the Li_2CO_3/K_2CO_3 electrolyte employed at high temperatures and 0.95 cm/S for the $Li_2CO_3/Na_2CO_3/K_2CO_3$ electrolyte employed in the lower temperature range, indicating that the strong discontinuity in resistance is due to the different cell configuration and, more specifically, the higher distance between the electrodes in the cell operating at lower temperature. This suggests that the performance of the process would improve significantly if it were operated with the planar geometry. On the other hand, the results obtained for the exchange current density suggest that the reaction mechanism is unaltered. This finding provides valuable insight for future, more detailed, modelling work as well as additional experimental investigations of the performance of MCECs at low temperatures.

4. Conclusions

A lab-scale MCEC operating at temperatures lower than 550°C was tested. The results obtained, along with those available in the literature for a cell operating at higher temperatures, were analyzed with a 0D model accounting for Ohmic and activation overpotentials. The results revealed that the activation overpotentials varied with continuity as a function of temperature, regardless of the electrolyte composition or cell geometry. These observations suggest that the electrochemical reaction mechanism does not depend on the electrolyte composition and that Ohmic losses play a significant role in the performance of MCECs, setting the basis for the future development of more detailed models and providing useful information to direct additional experimental investigation of MCECs.

Acknowledgments

The present activity was carried out under the collaboration agreement between the Dipartimento di Ingegneria Chimica Materiali Ambiente (DICMA) of the University of Rome “Sapienza” and the Italian National Agency for New Technologies, Energy and Sustainable Economic Development (ENEA) funded by the Italian Ministry of the Economic Development (MISE) under the “PIANO TRIENNALE 2019–2021 DELLA RICERCA DI SISTEMA ELETTRICO NAZIONALE”, PAR 2019, Research Topic “Power to Gas” of the “Sistemi di accumulo, compresi elettrochimico e power to gas, e relative interfacce con le reti” area.

References

Audasso E., Kim K.I., Accardo G., Kim H.S., Yoon, S.P, 2022, Investigation of molten carbonate electrolysis cells performance for H2 production and CO2 capture, Journal of Power Sources, 523, 231039.

Frangini S., Felici C., Tarquini P., 2013, A novel process for solar hydrogen production based on water electrolysis in molten carbonates, ECS Transactions, 61, 13.

Hauch A., Kungas R., Blennow P., Hansen A.B., Hansen J.B., Mathiesen B.V., Mogensen M.B., 2020, Recent advances in solid oxide cell technology for electrolysis, Science, 370, 186.

Hu L., 2016, Physical and chemical properties of molten carbonates, PhD Thesis, KTH Royal Institute of Technology, Stockholm, Sweden.

Kojima T, Miyakazi Y., Nomura K., Tanimoto K., 2008, Density, surface tension, and electrical conductivity of ternary molten carbonate system Li2CO3/Na2CO3/K2CO3 and methods for their estimation, Journal of the Electrochemical Society, 155, F150.

Monforti Ferrario A., Santoni F., Della Pietra M., Rossi M., Piacente N., Comodo G., Simonetti L., 2021, A system integration analysis of a molten carbonate electrolysis cell as an off-gas recovery system in a steam reforming process of an oil refinery, Frontiers in Energy Research, 9, 655195.

Perez-Trujillo P., Elizalde-Blancas F., Della Pietra M., McPhail S.J., 2018, A numerical and experimental comparison of single reversible molten carbonate cell operating in fuel cell mode and electrolysis mode, Applied Energy, 226, 1037-1055.

Reyes Belmonte M., Delgato A., Diaz E., Gonzalez-Aguilar J., Romero M., 2017, Molten carbonates electrolyzer model for hydrogen production coupled to medium/low temperature solar power plant, ISES Conference Proceedings, 01, 1-11.